JOURNAL OF GEOPHYSICAL RESEARCH, VOL. 99, NO. B5, PAGES 9035–9044, MAY 10, 1994

Micromagnetic modeling of two-dimensional domain structures in magnetite

Song Xu and David J. Dunlop

Department of Physics, Erindale College, University of Toronto, Mississauga, Ontario, Canada

Andrew J. Newell

Geophysics Program, University of Washington, Seattle

Abstract. Micromagnetic studies of two-dimensional domain structures in various local energy minimum states were carried out for 1- and 5-μm cubes of magnetite. Domain structures obtained for the cubes are relatively simple compared to ones from previous two- and three-dimensional calculations for smaller magnetite grains (Newell et al., 1993a; Williams and Dunlop, 1989, 1990). With an initially assumed one-dimensional lamellar structure, the final two-dimensional structure reveals the formation of closure domains at the grain surfaces. The magnetization directions in closure domains are found to be determined largely by the magnetostatic energy, rather than the magnetocrystalline anisotropy as normally expected. The number of body domains that gives the lowest-energy state for the 1-μm magnetite cube is 2, while the number for the 5-μm cube is 4. These are much smaller equilibrium numbers of domains than the 6 and 13 domains obtained from a one-dimensional model by Moon and Merrill (1985) and the 4 and 10 domains predicted from a quasi-two-dimensional analysis by Ye and Merrill (1991) for 1- and 5-μm cubes, respectively. The numbers of domains predicted are comparable to the numbers observed in magnetite grains of similar sizes.

Introduction

Micromagnetic theory has been very successful in providing new concepts such as local energy minimum (LEM) states and transdomain processes linking these states [*Moon and Merrill*, 1985; *Enkin and Dunlop*, 1987; *Williams and Dunlop*, 1990; *Newell et al.*, 1993a]. These concepts go some way toward explaining observations of metastable single-domain (SD) states of large grains [*Halgedahl and Fuller*, 1980] and changes in the number of domains in particular grains when they are cooled from the Curie temperature [*Halgedahl*, 1991]. Nevertheless, there remains a gap between observation and theory, in part because observations are made on large and nonideal grains, while theories model relatively small and defect-free grains. One conspicuous problem is that domain structures predicted by two- and three-dimensional micromagnetic theories for magnetite grains [*Williams and Dunlop*, 1989, 1990; *Newell et al.*, 1993a] appear to be more complex than observed [*Boyd*, 1986; *Heider et al.*, 1988; *Worm et al.*, 1991; *Özdemir and Dunlop*, 1993]. Moreover, there is a long-standing problem in rock magnetism that the number of domains predicted for a given grain size by theory is always significantly greater than observed [e.g., *Moon*, 1991].

Grain size plays an important role in the above problems. For example, complex domain structures obtained from theoretical modeling result largely from the magnetostatic effect associated with magnetic poles at grain surfaces. With an increase in grain size and hence in the volume/surface ratio, one expects this surface effect to diminish. The trend toward simpler domain structures with increasing grain sizes has been shown by *Williams and Dunlop* [1990] for $\leq$ 1-μm magnetite grains. However, because of the relatively low resolution of the model (each cubic grain modeled by William and Dunlop was divided into 12×12×12 cells of equal size), important features such as domain structures at the grain surfaces cannot be resolved. The importance of surface structures in determining the number of domains in a grain of given size has been demonstrated by *Ye and Merrill* [1991]. By allowing magnetization vectors near the grain surface to deviate from a one-dimensional structure, *Ye and Merrill* [1991] obtained a smaller number of domains than *Moon and Merrill* [1985] had found for a magnetite grain of the same size. However, the constraints imposed by *Ye and Merrill* [1991] on magnetic structures in the surface layers make their quasi-two-dimensional model incapable of exploring the possible formation of closure domains as expected in a cubic crystal of magnetite.

Paper number 94JB00137.
0148-0227/94/94JB-00137$05.00

In this paper we apply a fully two-dimensional micromagnetic model to magnetite grains with sizes of 1 and 5 μm. The model was developed by *Newell et al.* [1993a]. We will examine particularly the formation of closure domains and their effect on the equilibrium number of body domains in a grain when it is in its lowest-energy state.

Micromagnetic Model

In our model a magnetite cube with linear dimension a is divided into a two dimensional array of n cells, each having a cross section a^2/n and length a (Figure 1). The crystallographic orientation of the cube is chosen such that the z axis is along the [111] easy axis and the x-z plane is the ($\bar{1}10$) plane, which is energetically most favorable for 180° Bloch walls in magnetite [*Lilley*, 1950]. The direction $\mathbf{m_i}$ of magnetization in each cell is described by the polar angle θ_i and the azimuthal angle ϕ_i, giving

$$\mathbf{m_i} = \sin\theta_i \cos\phi_i \hat{\mathbf{x}} + \sin\theta_i \sin\phi_i \hat{\mathbf{y}} + \cos\theta_i \hat{\mathbf{z}} . \quad (1)$$

A magnetic structure of the cube is described by the values of $2n$ variables θ_i and ϕ_i (i from 1 to n), determined by minimizing the total magnetic energy E_T of the cube. E_T is the sum of the exchange energy E_e, the magnetostatic-self energy E_m, and the magnetocrystalline anisotropy energy E_a. Following *Newell et al.* [1993a], the expressions for E_e, E_m and E_a are:

$$E_e = Aa \sum_{i=1}^{n} \sum_{j} (1 - \mathbf{m_i} \cdot \mathbf{m_j}), \quad (2a)$$

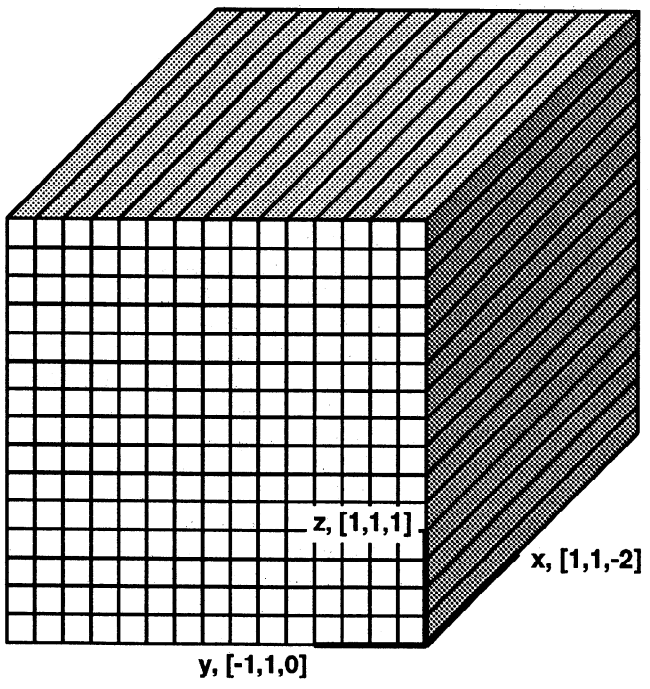

Figure 1. The subdivision of a cubic model grain into a two-dimensional array of cells and the crystallographic orientation of the cube used in the two-dimensional micromagnetic model.

$$E_m = \frac{\mu_0 a^3 M_s^2}{2n} \sum_{i,j=1}^{n} \mathbf{m_i} \cdot N_{ij} \cdot \mathbf{m_j}, \quad (2b)$$

$$E_a = K_1 a^3 \left[\frac{1}{n} \sum_{i=1}^{n} (\alpha_i^2 \beta_i^2 + \beta_i^2 \gamma_i^2 + \gamma_i^2 \alpha_i^2) - \frac{1}{3} \right], \quad (2c)$$

where A and K_1 are the exchange and magnetocrystalline anisotropy constants, respectively, M_s is the saturation magnetization, and μ_0 is the free-air magnetic permeability. In (2a), j is summed over nearest neighbours for each cell i. In (2b), N_{ij} is the magnetostatic interaction tensor between cells i and j [*Newell et al.*, 1993b]. It is a function of the relative positions of cells i and j for the given geometry in Figure 1. In (2c), α_i, β_i, and γ_i are the direction cosines of $\mathbf{m_i}$ with respect to the three <100> crystal axes. They can be related to θ_i and ϕ_i for a chosen crystal orientation (see Appendix A). The constant term $-K_1 a^3/3$ in (2c) is the magnetocrystalline anisotropy energy when the $\mathbf{m_i}$ directions are along a <111> easy axis. The magnetoelastic energy will not be considered in this study.

The conjugate gradient method [*Press et al.*, 1986] was used to achieve the minimization of E_T. The method begins with an initially guessed structure θ_{i0} and ϕ_{i0} and then iterates towards a lower-energy structure by using the first derivatives of E_T to determine the search direction. A detailed description of the minimization procedure is given in Appendix B. Two types of initial structures were used in this study: The first is a vortex structure with $\theta_{i0} = \tan^{-1}(z/y)$ and $\phi_{i0} = \pi/2$, where the origin is at the center of the cube. The second is a one-dimensional lamellar structure (with $\mathbf{m_i}$ in the x-z plane) with walls of zero width placed at the positions determined from the one-dimensional model of *Xu and Merrill* [1990].

The success of the minimization of E_T in a computation was assessed by using the self-consistency parameter S [*Newell et al.*, 1993a], defined as

$$S = \frac{\sum_{i=1}^{n} |\mathbf{m_i} \cdot \mathbf{H_i}|}{\sum_{i=1}^{n} |\mathbf{H_i}|}, \quad (3)$$

where $\mathbf{H_i}$ is the effective field given by

$$\mathbf{H_i} = -\frac{1}{\mu_0 V M_s} \frac{\partial E_T}{\partial \mathbf{m_i}}. \quad (4)$$

At equilibrium, $\mathbf{m_i} \times \mathbf{H_i} = 0$ (i.e., $\mathbf{m_i}$ aligns with $\mathbf{H_i}$) [*Brown*, 1963], and therefore $S = 1$. In an actual computation, S is always < 1.

The material constants used for magnetite in the model were $A = 1.32 \times 10^{-11}$ J/m, $M_s = 480$ kA/m, and $K_1 = -1.25 \times 10^4$ J/m^3. The number of cells used for a 1-μm magnetite cube was 50×50 and for a 5-μm cube was 100×100. The corresponding cell widths are $a/\sqrt{n} = 0.02$ and 0.05 μm for the 1- and 5-μm cubes, respectively. The self-consistency factor, S, was found to be > 0.99 for all structures determined for a 1-μm cube and > 0.92 for a 5-μm cube. The lower S value for the 5-μm cube is apparently due to the larger cell size.

Domain Structures in a 1-μm Magnetite Cube

A 1-μm magnetite cube was modeled with initially guessed vortex, single-domain, two-domain and three-domain structures (Figure 2). In order to give a simple presentation of the overall domain picture, we have plotted for each structure a 25 × 25, instead of a 50 × 50, array of arrows, each arrow representing the projection in the y-z plane of $\mathbf{m_i}$ averaged over four adjacent cells. In all cases the x component of $\mathbf{m_i}$ is very small except in Bloch walls.

With an initially guessed vortex structure the final structure (Figure 2a) resembles a four-closure-domain structure, but with Néel walls instead of Bloch walls. The structure gives a very small magnetostatic energy $E_m/E_{m0} = 0.061$, where $E_{m0} = \mu_0 M_s^2 a^3/6$ is the magnetostatic energy for an SD structure. The resulting total energy of the cube is $E_T/E_{m0} = 0.093$.

The final structure developed from an initially guessed SD structure consists of a large body domain with the $\mathbf{m_i}$ directions along the easy axis and four closure domains at the corners (Figure 2b). The formation of the closure domains reduces the magnetostatic energy to about half of that for a SD structure, at the expense of an increase in the wall energy. The resulting total energy of the cube, when normalized to E_{m0}, is 0.68. Because of the large body domain, the structure gives a relatively large saturation remanence ratio, M_{rs}/M_s, of 0.64, compared to 1.00 for the SD structure.

The structures shown in Figures 2c and 2d were obtained using initial lamellar two- and three-domain structures without closure domains. In both cases, two-dimensional closure domain structures develop at the top and bottom surfaces. It is interesting to note that the two-body-domain structure did not develop into a vortex structure which would give a lower energy ($E_T/E_{m0} = 0.15$ for the two-body-domain struc-

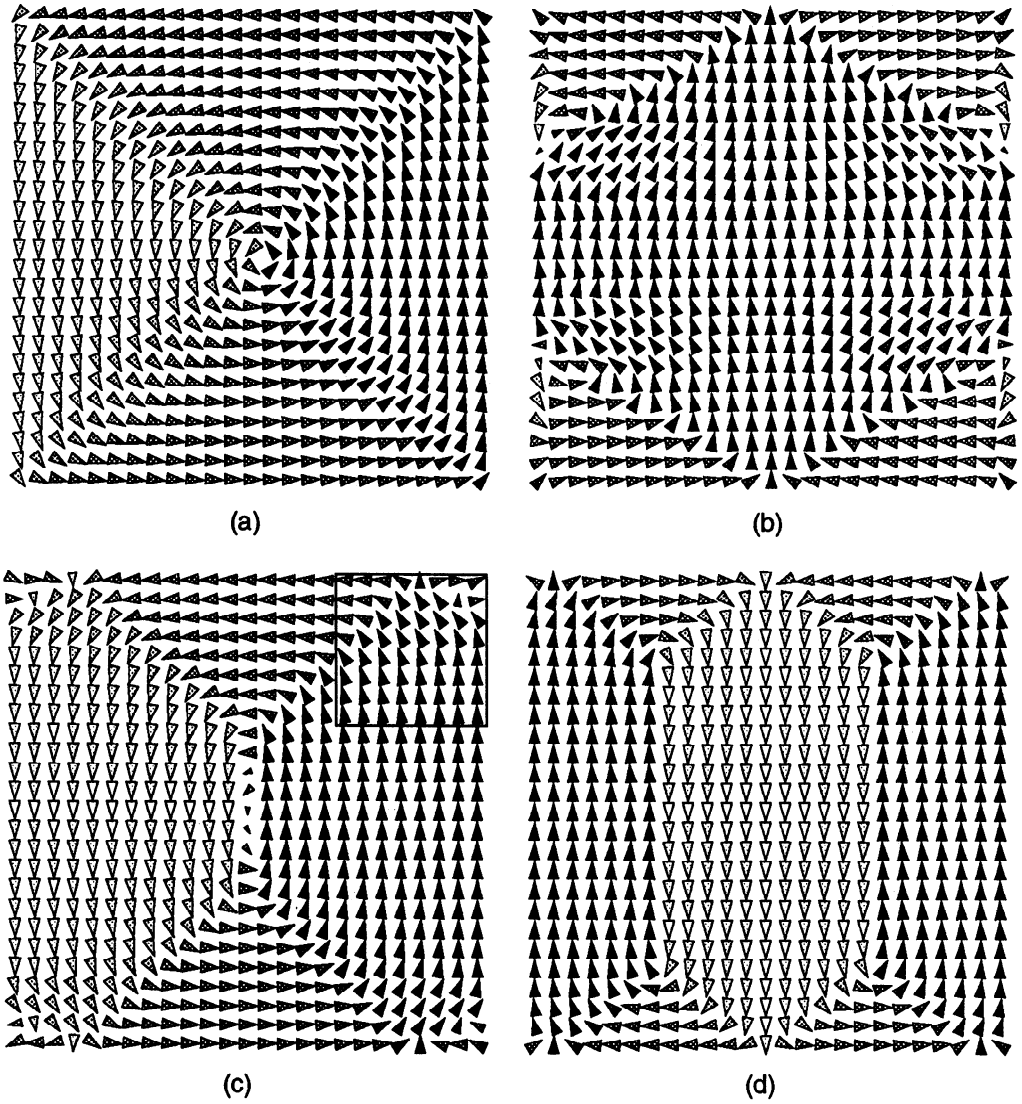

Figure 2. The two-dimensional domain structures determined for a 1-μm magnetite cube. The initially guessed structures used are (a) a vortex structure, (b) a single-domain structure, (c) a two-domain structure, and (d) a three-domain structure. The upper right corner area outlined in structure (c) is enlarged at a higher resolution in Figure 3.

ture, compared to 0.093 for the vortex structure in Figure 2a). This transformation is inhibited by the strong demagnetizing fields at the corners in the initial two-domain structure [see *Dunlop et al.*, 1990], which produce rotations of the $\mathbf{m_i}$ directions at the corners in a direction opposite to that needed to transform the two-domain structure into a vortex structure (Figure 2a). There is actually a small closure domain at each corner, as shown in Figure 3 by plotting the detailed structure of the upper right corner of the 50 × 50 array.

To test whether the two-body-domain structure shown in Figure 2c could transform to a vortex state when the corner domains are perturbed, we gave small perturbations, $\Delta\theta$, to the $\mathbf{m_i}$ directions in the four corner cells. The rotations of the $\mathbf{m_i}$ directions (by $\Delta\theta$) were chosen to be clockwise at the upper left and lower right corner cells and counterclockwise at the upper right and lower left corner cells, the most favorable rotations for transformation to a vortex state. When the $\mathbf{m_i}$ directions at individual corners were independently perturbed, there were a total 15 cases to be considered for a given $\Delta\theta$. For each case, the total energy E_T was reminimized while keeping the directions of the perturbed $\mathbf{m_i}$ directions fixed. The resulting changes in E_T are given in Appendix C for $\Delta\theta = 3°$ and 8°. In all cases the values of E_T increase, indicating that the structure in Figure 2c is stable against the given perturbations.

The closure domain structures shown in Figure 2 are not controlled by the magnetocrystalline anisotropy as normally expected. The magnetizations in the closure domains are parallel to the grain surfaces rather than along an easy axis. Apparently, these closure domains are controlled mainly by the magnetostatic energy. To ensure that this result is not a consequence of the chosen crystal orientation (Figure 1), in which there is only one easy axis in the viewing plane so that the 71° and 109° walls that form ideal closure domains are not actually energetically favored, we have calculated structures using different crystal orientations. One orientation puts the x axis in the [$\bar{1}$10] direction such that the viewing plane now contains the two easy axes [111] and [11$\bar{1}$], and the other puts the cube edges along the three <100> axes, respectively. The resulting structures obtained for these two cases were not noticeably different from those shown in Figure 2. Two examples are described in Appendix D for a 1-μm cube with the edges along the <100> axes.

We have also calculated domain structures using initial one-dimensional structures of four to six domains. In all cases, two-dimensional closure domain structures develop at the top and bottom surfaces, similar to those shown in Figures 2c and 2d. With an increasing number of body domains the size of the closure domains decreases, but the shape of the closure domains remains almost the same. *Ye and Merrill* [1991] also found that the thickness of the surface layer where the deviation from a one-dimensional structure occurs is inversely proportional to the number of domains in a grain of given size.

The minimized energies for the two-dimensional structures determined in this study for a 1-μm magnetite cube are compared in Figure 4 to those obtained by *Moon and Merrill* [1985] using a one-dimensional model. Among the two-dimensional structures, the vortex or four-closure-domain-like structure has the lowest E_T. The next lowest is the structure with two body domains, which is a considerably smaller number than the six domains in the lowest-energy state obtained by *Moon and Merrill* [1985] or the four domains obtained by *Ye and Merrill* [1991] using a quasi-two-dimensional calcu-

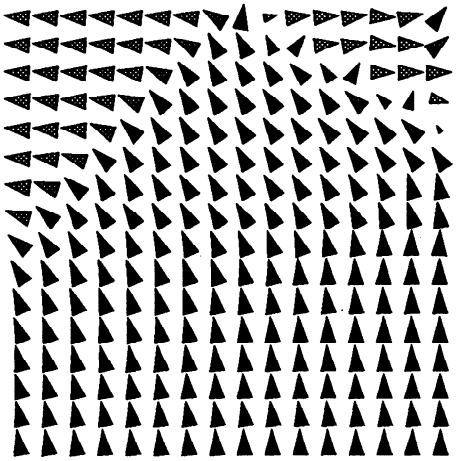

Figure 3. A high-resolution picture showing the detailed structure of the upper right corner of a 1-μm magnetite cube with two body domains (Figure 2c). The 16 × 16 array plotted covers about 10% of the area of the full 50 × 50 array.

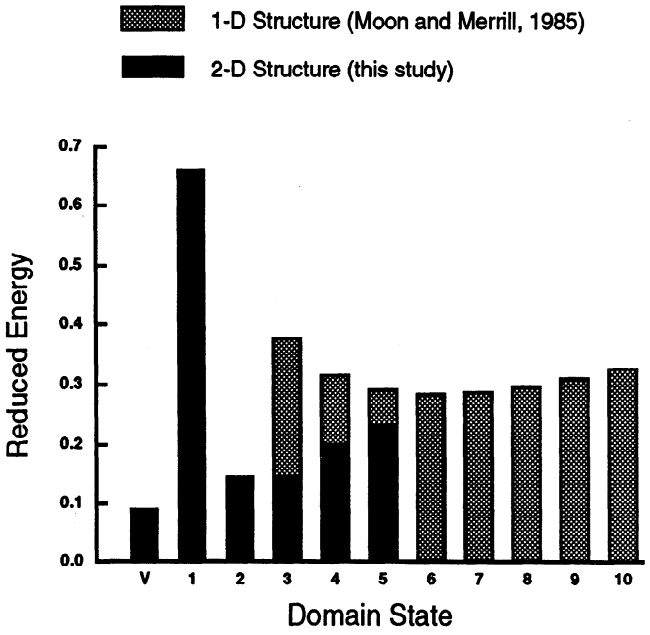

Figure 4. The minimized total energy E_T, normalized to the SD energy $\mu_0 M_s^2 a^3/6$, for a 1-μm magnetite cube in comparison with the results obtained by *Moon and Merrill* [1985] using a one-dimensional model. On the horizontal axis, V denotes the vortex state and the numbers refer to the number of body domains.

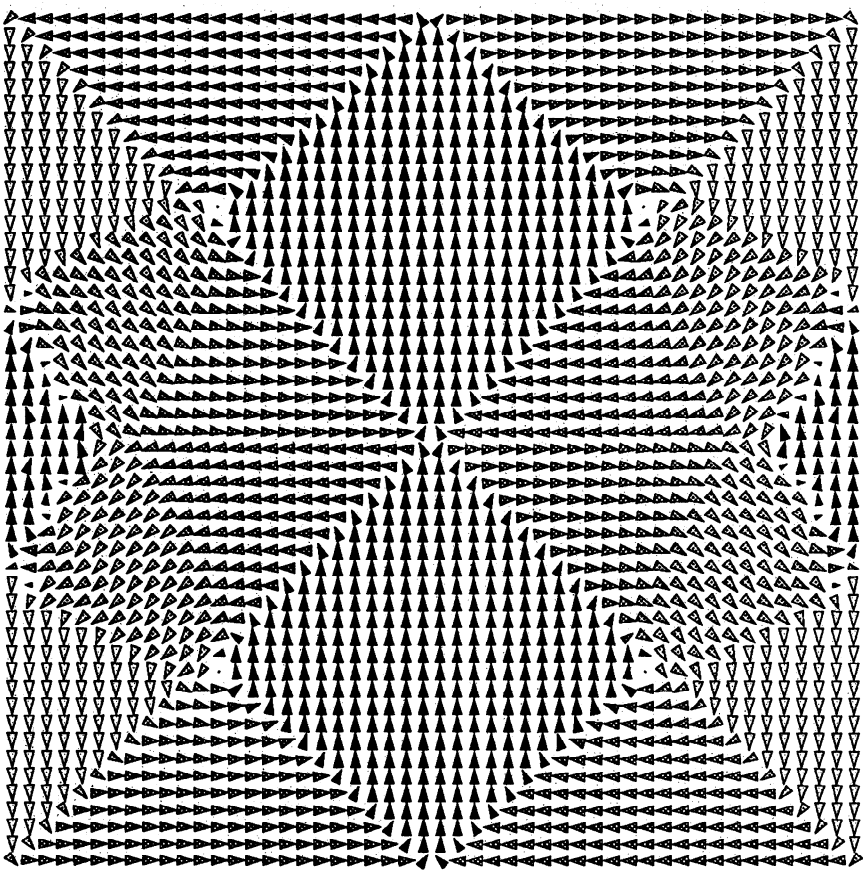

Figure 5. A checkerboardlike domain structure for a 5-μm magnetite cube. The structure was determined using an initial single-domain (SD) structure and is in a sharp contrast to the 1-μm one-body-domain structure (Figure 2b) determined also using an initial SD structure.

lation. In fact, the two-domain state was not even a permitted LEM state according to Moon and Merrill's calculations.

In Figure 4 the difference in the minimized energies between the one- and two-dimensional structures decreases with an increasing number of body domains. This decrease occurs because the size of the closure domains decreases and the two-dimensional structure approaches a one-dimensional structure. It should also be pointed out that the energy we determined for the six-body-domain structure (not shown) is actually slightly higher than that for the six-domain structure given by *Moon and Merrill* [1985]. The energies calculated by *Moon and Merrill* [1985] are underestimates because they used too small a value of the exchange constant: $A = 0.67 \times 10^{-11}$J/m [*Moskowitz and Halgedahl*, 1987].

Domain Structures in a 5-μm Magnetite Cube

We determined magnetic structures for a 5-μm magnetite cube using an initial vortex structure, and lamellar structures of one to six domains. Calculations were made using a 100×100 array but each structure is plotted as a 50×50 array of arrows, each representing the projection of $\mathbf{m_i}$ averaged over 4 adjacent cells.

Of particular interest is a checkerboardlike domain structure obtained using an initial SD structure (Figure 5). Unlike other structures, there is not much resemblance of the structure in Figure 5 to an initial SD structure. The structure can be viewed as consisting of four vortices and two small side domains. Because of the vortex formation, the structure gives a very low saturation remanence ratio, $M_{rs}/M_s = 0.024$ (in the z direction), compared to $M_{rs}/M_s = 0.64$ for the 1-μm, one-body-domain structure in Figure 2b, also obtained using an initial SD structure.

Other structures obtained using initial lamellar structures with the number of domains varying from two to six reveal well-formed closure domains at the grain surfaces. Three examples are shown in Figure 6. The magnetization directions in the closure domains are always parallel to the grain surface, thus indicating that these closure domains are controlled mainly by the magnetostatic energy instead of the magnetocrystalline anisotropy energy, as in the case of the 1-μm cube.

In both three- and four-body-domain structures (Figures 6a and 6b), a small vortex forms at each corner. This vortex formation is caused by corner demagnetizing fields in an initial one-dimensional structure, as in the case of corner domains in the 1-μm, two-body-domain structure (Figures 2c and 3). It should be pointed out that the apparently broad outermost walls

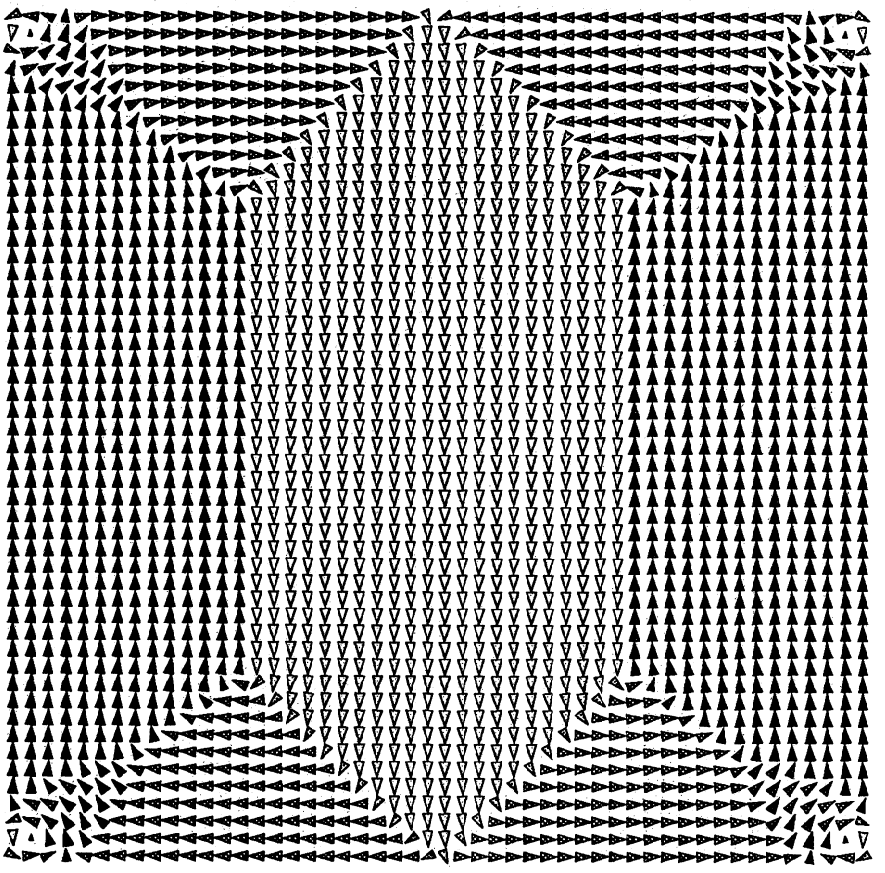

(a)

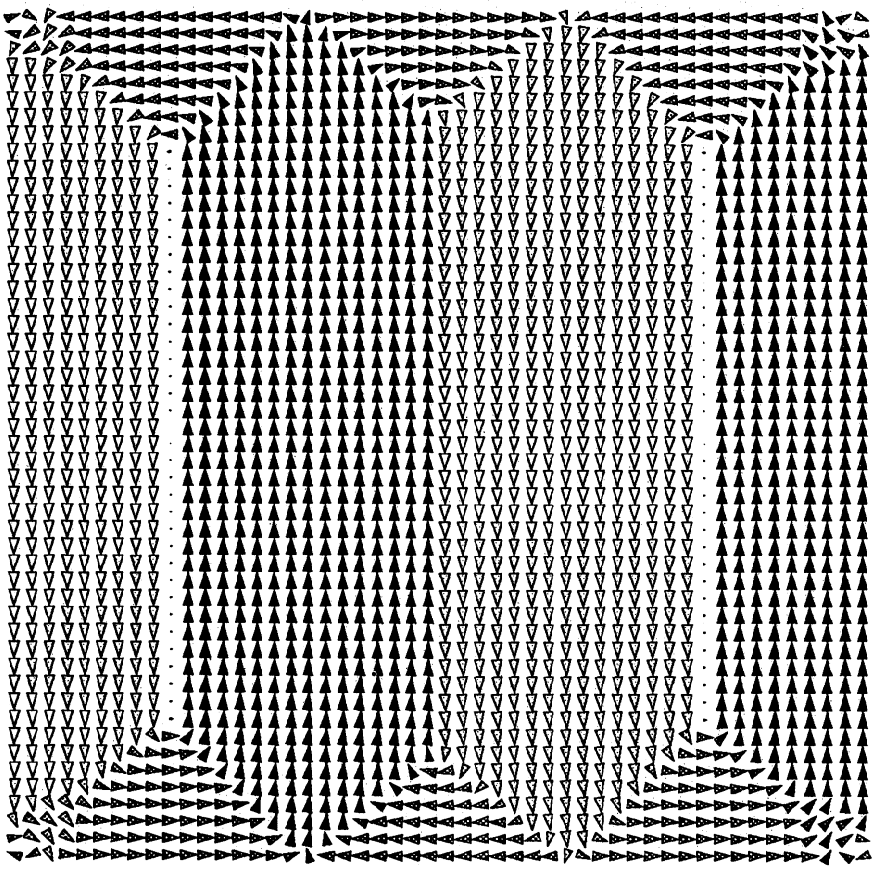

(b)

Figure 6. The closure domain structures determined for a 5-μm magnetite cube. The initial one-dimensional structures used are (a) three domains, (b) four domains, and (c) five domains.

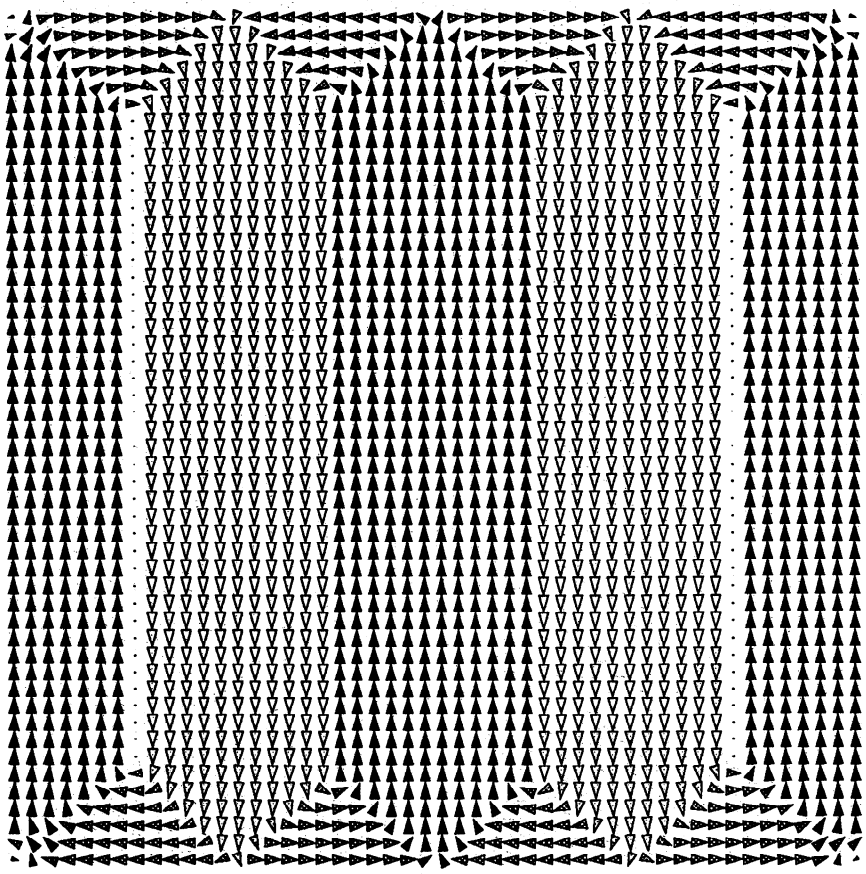

(c)

Figure 6. (continued)

seen in the four- and five-body-domain structures in Figures 6b and 6c are artifacts resulting from the averaging in adjacent cells of magnetization directions that are nearly antiparallel to each other.

The minimized energies for the two-dimensional structures determined for the 5-μm cube of magnetite are shown in Figure 7. The vortex structure, which has almost the same features as the one in Figure 2a, gives the lowest E_T. The next lowest is the structure with four body domains, which is much fewer than the 13 domains obtained by *Moon and Merrill* [1985] using a one-dimensional model and 10 domains calculated by *Ye and Merrill* [1991] using a quasi-two-dimensional model.

Discussion and Conclusion

The domain structures obtained from this study for both 1- and 5-μm magnetite cubes are simpler than those from previous two- and three-dimensional calculations for smaller grains [*Williams and Dunlop*, 1989, 1990; *Newell et al.*, 1993a]. Our results thus confirm the earlier speculation [*Williams and Dunlop*, 1990] that domain structures should become simpler when the grain size is larger.

The complexity of a final domain structure can vary greatly depending both on the initially guessed struc-

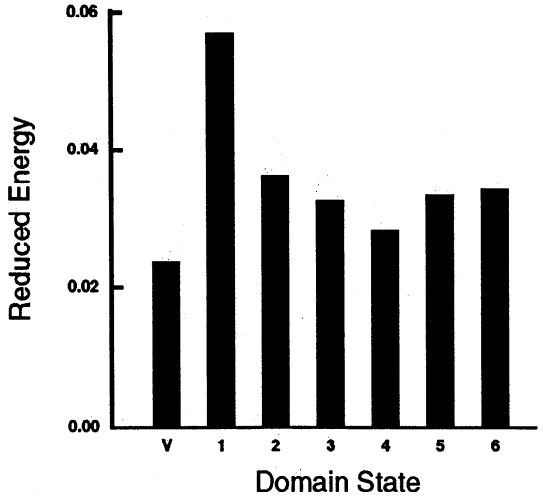

Figure 7. The variation in the minimized total energy E_T for various local energy minimum states in a 5-μm magnetite cube. The value of E_T has been normalized to the SD energy $\mu_0 M_s^2 a^3/6$. Among all the structures, the vortex structure, denoted by V on the horizontal axis, gives the lowest energy. The next lowest is the four-body-domain structure.

ture and grain size. One interesting example is to compare the relatively simple structures shown in Figure 2 with the complex multivortex structure obtained, also for a 1-μm magnetite cube, by *Newell et al.* [1993a] using almost the same micromagnetic model. In their study the initial structure for a given grain was taken to be the final structure determined for a grain of smaller size. Domain structures thus calculated at different grain sizes trace the change in magnetic structure during grain growth and are appropriate for modeling chemical remanent magnetization. In comparison, the structure shown in Figure 2b was determined using an initial simple SD structure and thus may resemble the saturation remanence state. An experimental demonstration of the variation of domain states for a grain after repeated acquisition of thermoremanent magnetization or alternating field demagnetization was given by *Halgedahl* [1991].

Grain size can also affect the complexity of a final domain structure. For example, compare the one-body-domain structure for the 1-μm cube (Figure 2b) with the relatively complex structure for the 5-μm cube (Figure 5), both determined using an initial SD structure.

The one-body-domain structure in a 1-μm cube in Figure 2b is important, because if it exists, it can contribute a large fraction of the remanent magnetization. The structure resembles a metastable SD state that has been observed sometimes in titanomagnetite grains tens of micrometers in size [*Halgedahl and Fuller*, 1980, 1983]. Our calculation indicates, however, that such a structure is unstable in a 5-μm cube of magnetite.

By allowing deviations from a one-dimensional structure, the numbers of body domains in the lowest energy state (excluding the vortex state) for 1- and 5-μm magnetite cubes are found to be 2 and 4, compared to 6 and 13 domains from a one-dimensional calculation [*Moon and Merrill*, 1985] and 4 and 10 domains from a quasi-two-dimensional calculation [*Ye and Merrill*, 1990], respectively. The number predicted for the 1-μm cube is comparable to the numbers observed for magnetite grains of similar sizes [*Smith*, 1980; *Morgan and Smith*, 1981]. The number of domains predicted for the 5-μm cube falls on the trend of the number of domains versus grain size observed for magnetite [e.g., *Boyd*, 1986; *Heider et al.*, 1988; *Worm et al.*, 1991]. No direct comparison can be made for the 5-μm cube because of the lack of domain observations for magnetite grains around 5 μm in size.

Closure domains are well developed in the structures determined for the 1- and 5-μm cubes. The directions of magnetization in the closure domains are controlled largely by the magnetostatic energy, rather than by the magnetocrystalline anisotropy. Magnetostatic control of closure domains is revealed by magnetization directions that are parallel to the grain surface instead of being along an easy axis. *Özdemir and Dunlop* [1993] recently have reported observations of well-formed closure domains in a single crystal of magnetite about 3 mm in size.

Among the structures investigated for the 1- and 5-μm magnetite cubes, the vortex structure gives the lowest energy. *Worm et al.* [1991] estimated that a vortex-like four-closure-domain structure should be the lowest-energy state for cubic magnetite grains in the entire MD size range. However, the vortex structure has never been observed for magnetite. One possible explanation is that the structure may be mistaken for a SD structure, because the "walls" in a vortex structure may not image well. Alternatively, a vortex structure may be suppressed as a result of the uniaxial anisotropy induced by macrostress, as suggested by *Worm et al.* [1991].

Appendix A: Transformation of a Magnetization Vector Between Two Coordinate Systems

For the crystal orientation chosen in Figure 1 the unit vectors of the x, y, and z axes are related to the unit vectors $\hat{\mathbf{i}}$, $\hat{\mathbf{j}}$, and $\hat{\mathbf{k}}$ along the three <100> axes by

$$\begin{bmatrix} \hat{\mathbf{x}} \\ \hat{\mathbf{y}} \\ \hat{\mathbf{z}} \end{bmatrix} = \begin{bmatrix} 1/\sqrt{6} & 1/\sqrt{6} & -2/\sqrt{6} \\ -1/\sqrt{2} & 1/\sqrt{2} & 0 \\ 1/\sqrt{3} & 1/\sqrt{3} & 1/\sqrt{3} \end{bmatrix} \cdot \begin{bmatrix} \hat{\mathbf{i}} \\ \hat{\mathbf{j}} \\ \hat{\mathbf{k}} \end{bmatrix}. \quad (5)$$

Thus a magnetization vector $\mathbf{m_i}$ in (1), which is expressed in the xyz system, has direction cosines

$$\alpha_i = \frac{1}{\sqrt{6}} \sin\theta_i \cos\phi_i - \frac{1}{\sqrt{2}} \sin\theta_i \sin\phi_i + \frac{1}{\sqrt{3}} \cos\theta_i,$$

$$\beta_i = \frac{1}{\sqrt{6}} \sin\theta_i \cos\phi_i + \frac{1}{\sqrt{2}} \sin\theta_i \sin\phi_i + \frac{1}{\sqrt{3}} \cos\theta_i,$$

and

$$\gamma_i = -\frac{2}{\sqrt{6}} \sin\theta_i \cos\phi_i + \frac{1}{\sqrt{3}} \cos\theta_i, \quad (6)$$

with respect to the three <100> axes.

Appendix B: Implementation of the Conjugate Gradient Method

In implementing the conjugate gradient method an important parameter to set is the step length s of the initial line search. In the computation we always began by setting s equal to E_T divided by the magnitude, $|G|$, of the gradient of E_T. Once $|G|$ was reduced below a specified value, the value of s was reduced successively to 0.1 and 0.01 of $E_T/|G|$, where E_T and $|G|$ are the minimized energy and the corresponding gradient in a previous s step. This process (with s varying from 1 to 0.1 to 0.01 of $E_T/|G|$) was repeated three times. The third time, s was further reduced to 0.001 and then 0.0001 of $E_T/|G|$, giving the final reduction in E_T in two successive iterations less than 0.0001 percent. For each new value of s the routine was restarted. We found that going back to a large value of s helped reduce E_T effectively. Other than that, our implementation uses a smaller step length of the line search when E_T is closer

Table 1. Fractional Changes in the Total Energy E_T When the Magnetization Directions in the Corner Cells of the Structure in Figure 2c are Perturbed by Angle $\Delta\theta$

Number of Cells Perturbed	Number of Cases Considered	Change in E_T	
		$\Delta\theta = 3°$	$\Delta\theta = 8°$
1	4	0.015 – 0.017	0.050 – 0.054
2	6	0.033 – 0.035	0.102 – 0.108
3	4	0.050 – 0.052	0.156 – 0.161
4	1	0.069	0.212

to the minimum. The computation for a 1-μm cube was carried on a Sun workstation and each structure took several hours of CPU to complete. In contrast, the computation for a 5-μm cube was carried out on a KSR parallel computer (using 18 processors), and each structure took about 15 hours to complete.

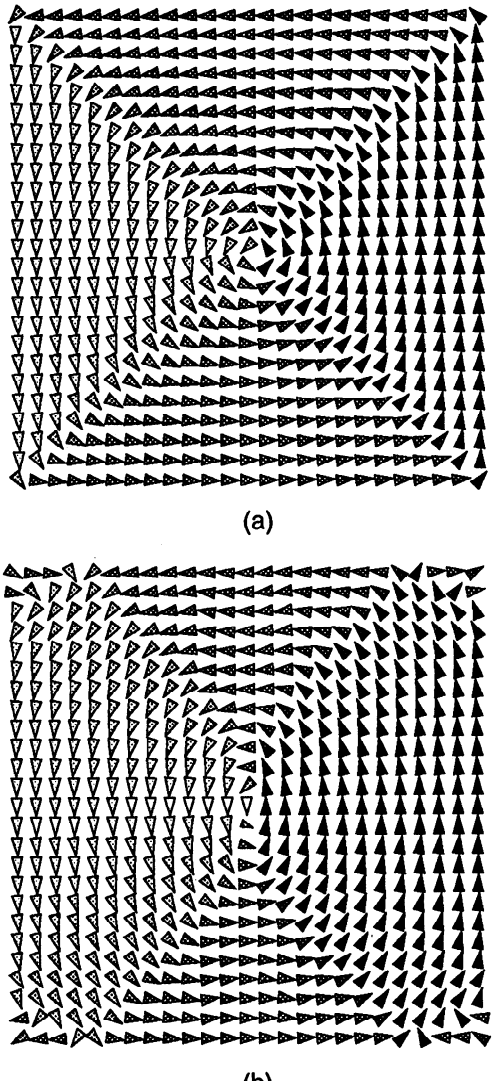

Figure 8. The two-dimensional domain structures determined for a 1-μm magnetite cube with its edges along the three <100> axes. The initially guessed structures used are (a) a vortex structure and (b) a two-domain lamellar structure.

Appendix C: Testing the Stability of the Two-Body-Domain Structure in a 1-μm Cube

Fractional changes in E_T are listed in Table 1, when the magnetization directions in the four corner cells in the structure shown in Figure 2c are independently perturbed by $\Delta\theta = 3°$ and 8°. There is a larger change in E_T when a larger number of corner cells are perturbed. In all cases, E_T increases with the given perturbations.

Appendix D: Two Structures in a 1-μm Cube With the Edges Along the <100> Axes

Figure 8 shows two structures obtained for a 1-μm magnetite cube with its edges along the three <100> axes, which are magnetically "hard" directions. They were obtained using initially guessed vortex and two-domain lamellar structures, respectively. In both cases the magnetizations in the closure domains are parallel to the grain surfaces, indicating that these closure domains are controlled mainly by the magnetostatic energy, rather than by the magnetocrystalline anisotropy energy. The structure shown in Figure 8a is similar to the vortex structure determined by *Newell et al.* [1993a] for a smaller magnetite cube. Note that the two body domains for the structure shown in Figure 8b are magnetized parallel to <100> hard directions and not along an easy axis. It is for this reason that the structure contains relatively larger closure domains than those shown in Figure 2c.

Acknowledgments. We have benefitted from the computer algorithm developed by Wyn Williams, discussions with Randy Enkin, and comments from Richard Reynolds and an anonymous reviewer. The manuscript has been substantially improved by the critical review of Wyn Williams. This research has been supported by NSERC operating grant A7709 to DJD.

References

Boyd, J. R., Domain observations on naturally occurring magnetite, M.S. thesis, 284 pp., Univ. of Calif., Santa Barbara, 1986.

Brown, W. F., Jr., *Micromagnetics*, 144 pp., John Wiley, New York, 1963.

Dunlop, D. J., R. J. Enkin, and E. Tjan, Internal field mapping in single-domain and multidomain grains, *J. Geophys. Res., 95,* 4561-4577, 1990.

Enkin, R. J., and D. J. Dunlop, A micromagnetic study of pseudo single-domain remanence in magnetite, *J. Geophys. Res., 92,* 12,726-12,740, 1987.

Halgedahl, S. L., Magnetic domain patterns observed on synthetic Ti-rich titanomagnetite as a function of temperature and in states of thermoremanent magnetization, *J. Geophys. Res., 96,* 3943-3972, 1991.

Halgedahl, S. L., and M.Fuller, Magnetic domain observations of nucleation processes in fine particles of intermediate titanomagnetite, *Nature, 288,* 70-72, 1980.

Halgedahl, S. L., and M. Fuller, The dependence of magnetic domain structure upon magnetization state with emphasis upon nucleation as a mechanism for pseudosingle domain behavior, *J. Geophys. Res., 88,* 6505-6522, 1983.

Heider, F., S. L. Halgedahl, and D. J. Dunlop, Temperature dependence of magnetic domains in magnetite crystals, *Geophys. Res. Lett., 15,* 499-502, 1988.

Lilley, B. A., Energies and widths of domain boundaries in ferromagnetics, *Philos. Mag., 41,* 792-813, 1950.

Moon, T. S., Domain states in fine particle magnetite and titanomagnetite, *J. Geophys. Res., 96,* 9909-9923, 1991.

Moon, T., and R. T. Merrill, Nucleation theory and domain states in multidomain magnetic material, *Phys. Earth Planet. Inter., 37,* 214-222, 1985.

Morgan, G. E., and P. P. K. Smith, Transmission electron microscopy and rock magnetic investigations of remanence carriers in a Precambrian metadolerite, *Earth Planet. Sci. Lett., 53,* 226-240, 1981.

Moskowitz, B. W., and S. L. Halgedahl, Theoretical temperature and grain-size dependence of domain state in x=0.6 titanomagnetite, *J. Geophys. Res., 92,* 10,667-10,682, 1987.

Newell, A. J., D. J. Dunlop, and W. Williams, A two-dimensional micromagnetic model of magnetizations and fields in magnetite, *J. Geophys. Res., 98,* 9533-9549, 1993a.

Newell, A. J., W. Williams, and D. J. Dunlop, A generalization of the demagnetizing tensor for non-uniform magnetization, *J. Geophys. Res., 98,* 9551-9555, 1993b.

Özdemir, Ö., and D. J.Dunlop, Magnetic domain structures on a natural single crystal of magnetite, *Geophys. Res. Lett., 20,* 1835-1838, 1993.

Press, W. H., B. P. Flannery, S. A. Teukolsky, and W. T. Vetterling, *Numerical Recipes,* 702 pp., Cambridge University Press, New York, 1986.

Smith, P. P. K., The application of Lorentz electron microscopy to the study of rock magnetism, *Inst. Phys. Conf. Ser., 52,* 125-128, 1980.

Williams, W., and D. J. Dunlop, Three-dimensional micromagnetic modeling of ferromagnetic domain structure, *Nature, 337,* 634-637, 1989.

Williams, W., and D. J. Dunlop, Some effects of grain shape and varying external magnetic fields on the magnetic structure of small grains of magnetite, *Phys. Earth Planet. Inter., 65,* 1-14, 1990.

Worm, H.-U., P. J. Ryan, and S. K. Banerjee, Domain size, closure domains, and the importance of magnetostriction in magnetite, *Earth Planet. Sci. Lett., 102,* 71-78, 1991.

Xu, S., and R. T. Merrill, Thermal variation of domain wall thickness and number of domains in magnetic rectangular grains, *J. Geophys. Res., 95,* 21,433-21,440, 1990.

Ye, J., and R. T. Merrill, Differences between magnetic domain imaging observations and theory, *Geophys. Res. Lett., 18,* 593-596, 1991.

D. J. Dunlop and S. Xu, Department of Physics, Erindale College, University of Toronto, Mississauga, Ontario, Canada, L5L 1C6.

A. J. Newell, Geophysics Program AK-50, University of Washington, Seattle, WA 98195.

(Received April 26, 1993; revised December 29, 1993; accepted January 13, 1994.)